Title

Mesoscale electric fluctuations interacting with zonal flows, magnetic fluctuations and turbulence

Journal

Nuclear Fusion, 57(7)

ISSN

0029-5515

Authors

Zhao, KJ
Nagashima, Y
Diamond, PH
et al.

Publication Date

2017-07-01

DOI

10.1088/1741-4326/aa6f35

Mesoscale electric fluctuations interacting with zonal flows, magnetic fluctuations, and turbulence

K. J. Zhao,[1] Y. Nagashima,[2] P. H. Diamond,[3] J. Q. Dong,[1, 4] K. Itoh,[5] S.- I. Itoh,[2] L. W. Yan,[1] J. Cheng,[1] A. Fujisawa,[2] S. Inagaki,[2] Y. Kosuga,[2] M. Sasaki,[2] Z. H. Huang,[1] D. L. Yu,[1] Q. Li,[1] X. Q. Ji,[1] X. M. Song,[1] Y. Huang,[1] Yi. Liu,[1] Q. W. Yang,[1] X. T. Ding,[1] X. R. Duan[1] and HL-2A team[1]

1) *Southwestern Institute of Physics, P. O. Box 432, Chengdu, 610041， China*

2) Research Institute for Applied mechanics, Kyushu University, Kasuga, Kasuga koen 6-1, 816-8580, Japan

3) Center for Momentum Transport and Flow Organization, University of California at San Diego, California 92093, USA

4) Institute for Fusion Theory and Simulation, Zhejiang University, Hangzhou, 310027， China

5) National Institute for Fusion Science, Toki 509-5292, Japan

Abstract: New mesoscale electric fluctuations (MSEFs) are identified in the edge plasmas of the HL-2A tokamak using multiple Langmuir probe arrays. The MSEFs, resulting from the synchronization and having components of dominant GAM and m/n=6/2 potential fluctuations, are found at the same frequency as that of the magnetic fluctuations of m/n=6/2 (m and n are poloidal and toroidal mode numbers, respectively). The temporal evolutions of the MSEFs and the magnetic fluctuations clearly show the frequency entrainment and the phase lock between the GAM and the m/n=6/2 magnetic fluctuations. The results indicate that GAMs and magnetic fluctuations can transfer energy through nonlinear synchronization. The nonlinear coupling analyses show that the MSEFs couple to turbulence and low frequency zonal flows (LFZFs). This suggests that the MSEFs may contribute to the LFZF formation, reduction of turbulence level, and thus confinement regime transitions. The analysis

of the envelope modulation demonstrates that both the MSEFs and the LFZFs modulate the turbulence while the MSEFs are modulated by the LFZFs.

1. Introduction

Interaction of magnetic field structures and flows in magnetohydrodynamics is a subject of general interest in physics. Typical examples include magnetic braking of stellar rotation [1], angular momentum transport in astrophysical disks [2, 3], and dynamics of the Earth's core and geodynamo [4]. In fusion plasmas, the interactions between plasma flows and magnetic fluctuations have attracted attention, for understanding and control of plasma confinement and transport. For example, the neoclassical tearing modes, which need a seed magnetic island for onset [5, 6], can be, theoretically, triggered by a turbulence noise source [7]. At the same time, the magnetic island-induced sheared flows can suppress turbulence and contribute to the formation of an internal transport barrier [8]. The coupling of torioidal Alfven eigenmodes (TAEs) and Beta-induced Alfven eigenmodes (BAEs) to the zonal flows is predicted to reduce the saturation level of TAEs and BAEs so as to reduce fast ion loss [9]. For the mitigation or suppression of the large edge localized modes in the high confinement mode (H-mode) plasmas, which is considered to be an urgent task for fusion research, the resonant magnetic perturbations (RMPs) [10] are used worldwide. In applying RMPs, the interactions of magnetic perturbations, zonal flows [11], and microscopic turbulence take place.

Two types of zonal flows, (i.e., the low frequency zonal flows (LFZFs) [11, 12] and the geodesic acoustic modes (GAMs)[13, 14]), are known. The effects of magnetic perturbation on zonal flows were reported. For instance, the GAM is damped in the presence of RMPs [15]; the RMP-induced magnetic islands can enhance the LFZFs and turbulence，and accelerate the edge toroidal rotation [16,17]; the poloidal flows are reversed when the RMP-induced island width is large enough [18]; a quasi-coherent mode is detected near the low safety factor rational surface [19, 20]. However, the dynamical and mutual interaction between flows and magnetic perturbations has not been deeply studied experimentally.

To understand the complicated interaction of the flows with the magnetic structures, we have to know the ways of their interaction dynamically. Here, the observation of the synchronization, a universal nonlinear phenomenon in nature [21–24], of GAMs and magnetic fluctuations in the edge plasmas of the HL-2A tokamak is reported [25]. The frequency entrainment and phase lock, two essential elements in synchronization, are demonstrated. Because the magnetic field and velocity field are the two essential vector fields in plasmas, governing the turbulent structure formation in the Universe and laboratory, the discovery of synchronization reveals a new, essential and prototypical process in nonlinear dynamics of high temperature plasmas. The mesoscale electric field fluctuations (MSEFs), resulting from the synchronization, can interact with the LFZFs and turbulence through nonlinear three wave coupling. The mesoscale refers to the finite radial wavelength ~ L in the regime of r_c <L<a. Here, r_c and a are the correlation length of turbulence and macro-scale of the system. On the HL-2A tokamak, the r_c and a are ~0.5 cm and ~40 cm, respectively.

The rest of this work is organized as follows. The experimental set-up is given in section 2. The experimental results, described in section 3, include the observation of the MSEFs, the mode structures of the MSEFs, the frequency entrainment and the phase lock between the GAMs and magnetic fluctuations, and the nonlinear interaction among magnetic fluctuations, MSEFs, LFZFs, and turbulence etc. Section 4 presents the discussion and conclusion.

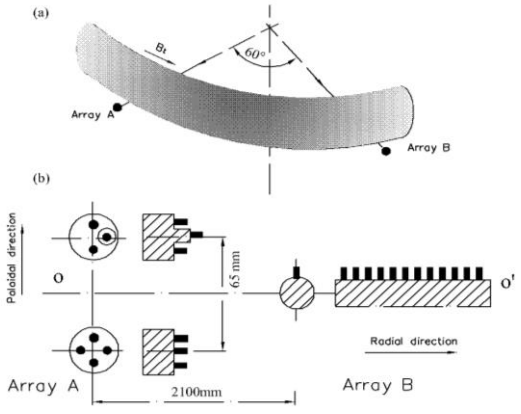

Fig. 1. (color online) Layout and structure of the LP arrays.

2. Experiment setup

The experiments presented here were conducted in Ohmic and electron-cyclotron-resonance-heating (ECRH)

deuterium plasmas of a circular cross section on the HL-2A tokamak. The major and minor radii of the HL-2A tokamak are R = 1.65 m and a = 0.4 m, respectively. The ECRH power is ~500 kW. The parameters specially set for the experiments are the toroidal magnetic field B_t = 1.2-1.3 T, the plasma current I_p = 150-180 kA, the line averaged electron density N_e = 1-2X10$^{19}m^{-3}$, the safety factor q_a = 3.3. The sampling rate of the probe data is 1 MHz corresponding to Nyquist frequency of 500 kHz. The frequency resolution is 0.25 kHz in the following analysis unless otherwise stated. A combination of distributed Langmuir probe (LP) arrays was used to measure floating potential fluctuations，and density and temperature profiles, as shown in the figure 1. In the combination, a LP array of three tips and a four-tip LP array form a fast reciprocating probe set of seven tips with a 65 mm poloidal span. A radial rake probe array of 12 tips, in the toroidal direction, is located in the poloidal cross section 2100mm away from the set of seven tips. It was used to get radial profiles of floating potential fluctuations. The tip size and the mount of the LP sets are the same as was described in Ref. [26].

3. Experiment results

3.1 Observations of MSEFs

The new mesoscale electric fluctuations with components of the dominant GAMs and the m/n=6/2 potential fluctuations are detected inside the last closed flux surface (LCFS) in ECRH plasmas. The tip is located at the radial position of Δr = -4.6cm, where the minus sign means inwards from the LCFS. Figures 2(a) and (b) give the auto power spectra of the floating potential fluctuations and the magnetic fluctuations from the Mirnov coils set up on the vacuum vessel wall, respectively. The small peak shown in

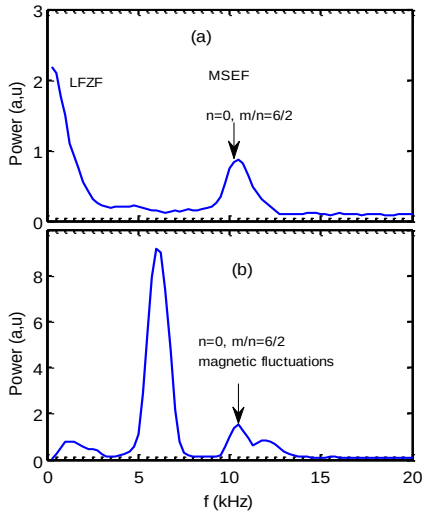

Fig. 2 (color online) The auto-power spectra of (a) the floating potential fluctuations and (b) the magnetic fluctuations.

the figure 2(a) at the frequency of ~10.5 kHz is the MSEF. A large power fraction peak of the LFZF in the frequency range of ~0.25-3 kHz was also detected. The large peak at the frequency of ~ 6 kHz shown in figure 2 (b) is the tearing modes with mode numbers of m/n=2/1. The small peak presented in figure 2(b) at the same frequency as the MSEFs has components of the dominant m/n=6/2 magnetic fluctuations and the n=0 zonal field. Besides, the two small peaks at the frequency of 1.2 kHz and 12 kHz come from the power supply and the m/n=4/2 tearing mode, respectively.

3.2 Mode structures of the MSEFs

Figures 3 (a)-(d) show the toroidal coherency between potential fluctuations, their phase shifts, the coherency between floating potential and magnetic fluctuations, and the radial phase shifts between potential fluctuations, respectively. The toroidal coherency in the LFZF and MSEF frequency bands is all quite high. This indicates that the MSEF and LFZF have strong correlation in the toroidal direction with a span of 2100 mm. The corresponding phase shift in the MSEF frequency region is estimated as $\Delta\phi_t = 0.25 \pm 0.09$ *rad*. The toroidal mode number is calculated as $n = 0 \pm 0.2$. The evaluated radial phase shift is $\Delta\phi_r = 1.4 \pm 0.2$ *rad* with a spans of 4 mm in radial direction, and the corresponding radial wave vector is estimated as $k_r = 3.5 \pm 0.2\ cm^{-1}$. Thus, we conclude that the MSEF has the characteristics of the toroidal symmetry, and finite radial wave numbers, and thus the GAM component is dominant. In addition, the calculated coherency between the MSEFs and the magnetic fluctuations at the MSEF frequency is significantly above

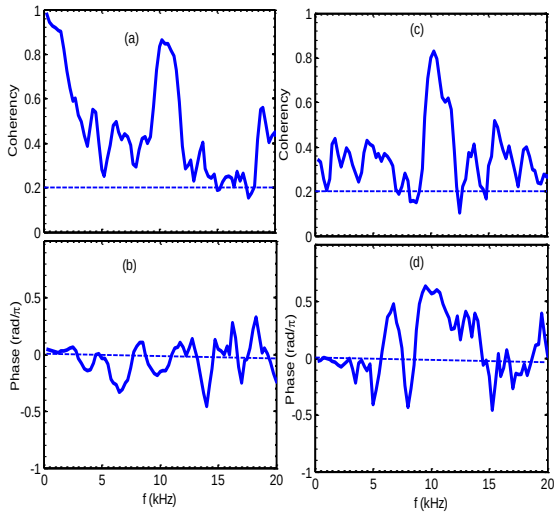

Fig .3. (color online) (a) The toroidal coherency between potential fluctuations, and (b) its toroidal phase shift, (c) the coherency between floating potential and magnetic fluctuations, and (d) the radial phase shift between potential fluctuations.

the noise level, indicating that the MSEFs are well correlated with the magnetic fluctuations.

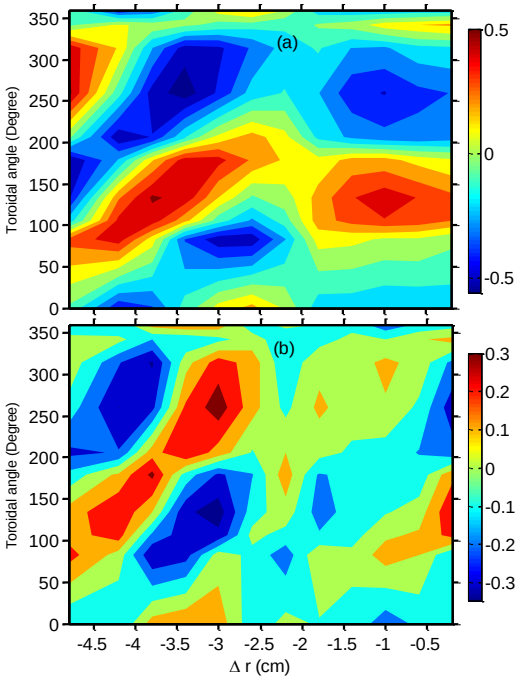

Fig. 4 (color online) The contour plots of coherency between potential and magnetic fluctuations (a), and between turbulence envelope and magnetic fluctuations in the frequency band of 9-11kHz (b).

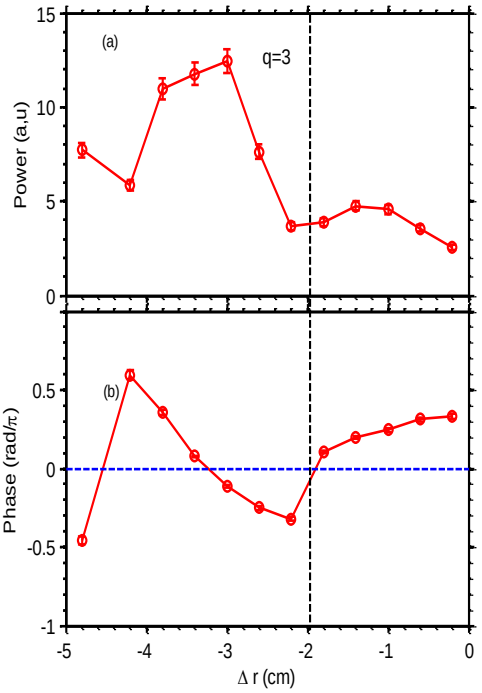

Fig. 5. (color online) The radial profiles of MSEF power (a), and the phase shift between potential and magnetic fluctuations of m/n=6/2 (b).

The spatial structures of the MSEF at the frequency of ~10.5 kHz were identified further with correlation analysis. Figure 4 (a) shows the contour of C(X(Δ r), Y(ξ)), where X(Δ r) is the potential perturbation at r = a+ Δ r and Y(ξ) is the magnetic fluctuation measured with the Mirnov coil at the toroidal angle ξ. Here, the coherency is described as $C_{XY} = \langle (X_i - X)(Y_i - Y) \rangle / [\sqrt{< (X_i - X)^2 >} \sqrt{< (Y_i - Y)^2 >}]$, where X_i and Y_i are two sets of variables, i stands for time series, and < ... > denotes an ensemble average, though in this work this was estimated from the data using a time average, i.e. by applying the ergodic hypothesis. X and Y are the averages of X_i and Y_i, respectively. The 12 probe tips are uniformly distributed in the radial direction from -4.8 to -0.4 cm inside the LCFS. The 10 Mirnov coils are located at different

toroidal angles. The toroidal mode number of n=2 is clearly demonstrated for the potential fluctuation at the frequency of ~10.5 kHz. The poloidal mode number of m=6 is also estimated with similar analysis. Figure 4 (b) also gives the contour plot of the coherency between turbulence envelopes [27] and magnetic fluctuations. The poloidal and toroidal mode numbers for the turbulence envelope are identified as m=6 and n=2, respectively. This analysis indicates that the MSEF also contains m/n=6/2 potential fluctuations. The phase shift between the turbulence envelope and the m/n=6/2 potential fluctuation is close to $\pi/2$. The radial wavelengths of the m/n = 6/2 potential fluctuation and turbulence envelope are all estimated as about ~2 cm. The m/n = 6/2 potential fluctuation propagates in the directions of toroidal magnetic field and ion diamagnetic drift.

The radial distributions of the potential fluctuation power at the MSEF frequency are measured and shown in figure 5 (a). The power as a function of the radial position shows two peaks. The amplitude of the MSEF first increases from the LCFS inwards, but reduces at the position of Δr~-2.0 cm, where the surface of the safety factor q=3 is located. Then the power increases again and reaches a maximum at Δr~ -3.0 cm. After that, the power deceases inwards. The profiles of the phase shift between the MSEFs and the magnetic fluctuations by Fast Fourier Transformation analysis is also provided in figure 5 (b). The sign of the phase shift changes at Δr ~ -2.0 cm, indicating that the sign of the MSEF inverts at the q=3 surface. The reduction of the MSEF and the change of the sign for the MSEF around q=3 surface may come from the m/n=6/2 islands. The radius of q=3 surface is estimated by magnetic measurements.

3.3 Time evolutions of MSEFs and magnetic fluctuations

In order to understand the interaction mechanism of the GAMs and the magnetic fluctuations, the temporal evolutions of the MSEFs and magnetic fluctuations of m/n=6/2 are investigated. Figure 6(a) shows the spectrogram of the floating potential fluctuations in the MSEF frequency range at the radial position of Δr=-3.0 cm. In the

period of 500 - 530 ms, the MSEF frequency rapidly decreases from 15.5 kHz to 12.5 kHz. At the beginning of the ECRH heating, the MSEF is located at the frequency of ~ 12.5 kHz, and its frequency decreases continuously. After ~590 ms, the MSEF frequency becomes stable and is about 10.5 kHz. Figure 6 (b) also gives the spectrogram of the m/n=6/2 magnetic fluctuations. The m/n=6/2 magnetic fluctuations follow the MSEF frequency and its intensity increases gradually. At 20 *ms* after the ECRH switching off, i.e., at ~650 *ms*, the MSEF frequency decrease again and no significant magnetic fluctuation is observed at the MSEF frequency. The result suggests that the frequency entrainment of the GAM and the m/n=6/2 magnetic fluctuations exists during the ECRH heating.

The temporal evolutions of the coherencies between the MSEFs at the radial position of Δr=-3.0 cm and magnetic fluctuations are provided in figure 6 (c). The coherency was calculated as $\gamma_{XY} = |C_{XY}|$. The time window is 5ms and the band pass filter of two signals is 9-16 kHz. The higher coherency suggests the existences of the stronger coupling between the MSEFs and the m/n=6/2 magnetic fluctuations. With ECRH heating, the increase of the coherency suggests that the coupling strength is enhanced, particularly, during 610-620 ms.

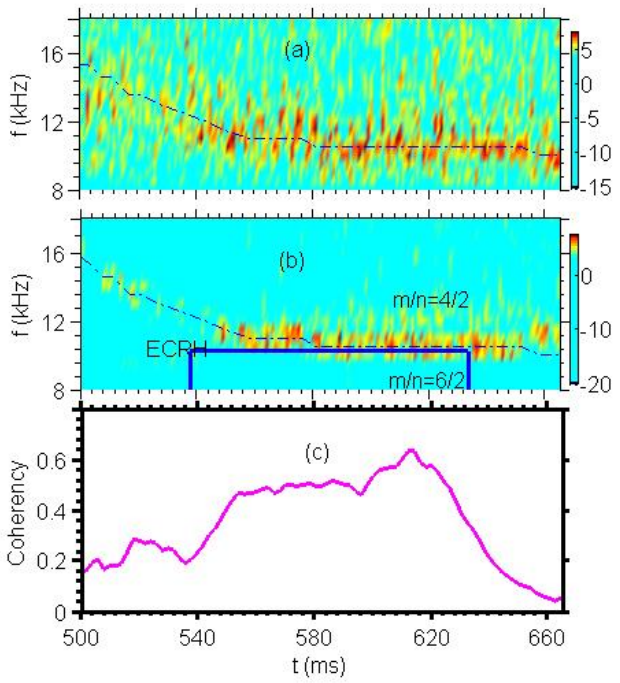

Fig.6. (color online) The spectrograms of the MSEFs (a) and magnetic fluctuations of m/n=6/2 (b), and the temporal evolution of the coherency between the MSEFs and magnetic fluctuations of m/n=6/2 (c). (The dash-dotted line indicates the evolution of the center of the MSEF frequency).

3.4 Phase lock between MSEFs and magnetic fluctuations

The phase lock is another important evidence to prove the frequency entrainment linked to the nonlinear synchronization of GAMs and magnetic fluctuations. Figure 7 shows the probability density function (PDF) of the phase shifts between MSEFs and magnetic fluctuations at different time slices. The phase shifts are estimated with the Hilbert transform. Before ECRH heating, no significant peak is observed at different time regions. This indicates that their phases are unlocked. After ECRH switching on, the peaks become significant and the half widths of the peaks become narrow, especially, during the periods of 600-610 and 610-620 ms. After ECRH switching off, the half widths of the peaks become wider and the peak disappears gradually. This result suggests that the phase shifts between GAMs and magnetic fluctuations are locked through adjusting their phases via nonlinear interaction during ECRH heating.

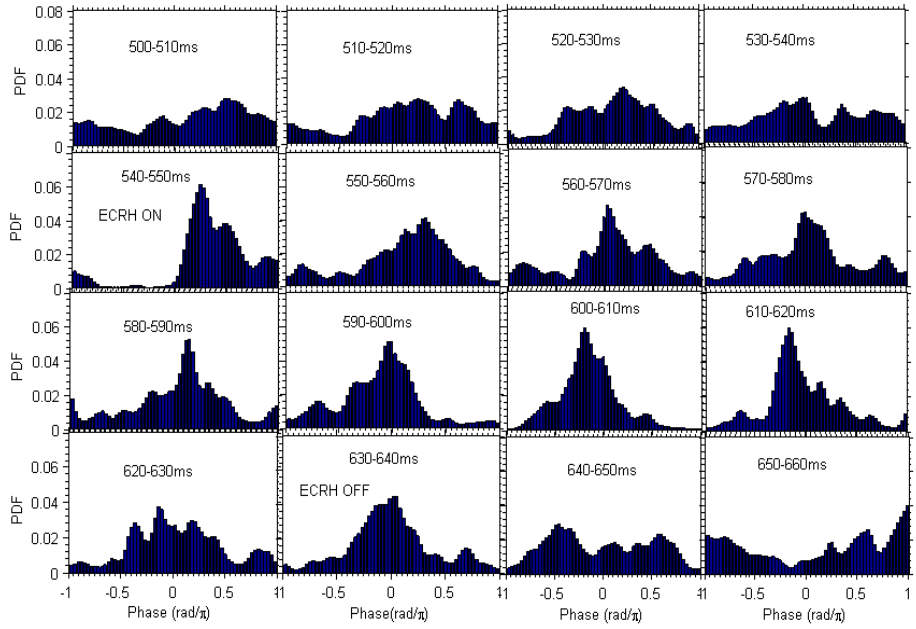

Fig. 7. (color online) The probability density functions of phase shifts between MSEFs and magnetic fluctuations at different time slices.

3.5 Nonlinear coupling of MSEFs and LFZFs to turbulence

The coupling of the LFZFs and MSEFs to turbulence is an important physics mechanism associated with LFZF and MSEF formation mechanism. The bicoherence analysis, an indicator for the strength of nonlinear three wave coupling, can be used to

prove the existence of the coupling of the LFZFs and MSEFs to turbulence. The squared auto-bicoherence $\hat{b}_f(f_3) = |B(f_3)|^2 / \left[\left\langle |\phi_f(f_1)\phi_f(f_2)|^2 \right\rangle \left\langle |\phi_f(f_3)|^2 \right\rangle \right]$ of the perturbations is calculated. Here the bispectrum $B(f_3) = \phi_f(f_1)\phi_f(f_2)\phi_f^*(f_3 = f_1 + f_2)$. The frequency resolution is 1 kHz. The number of realization is M=472, and the noise level is 0.002 for the analysis. Figure 8(a) plots the squared auto-bicohence of the floating potential fluctuations in the frequency region of f_1<100 kHz, and f_2=-100-+100 kHz. The bicoherence in the frequency region of f_1 = >60 *kHz*, f_2 = ~10.5*kHz*, and $f = f_1 + f_2$ ~ 10.5 *kHz* is significantly above the noise level. This analysis suggests that the turbulence may contribute to the MSEF formation through the nonlinear three wave coupling. In addition, the values of the bicoherences in the frequency region of f_1 <=60 *kHz*, f_2 = ~0-4*kHz*, and $f = f_1 + f_2$ ~ 0-4*kHz* are higher. This indicates that the turbulence may also contribute to the LFZF formation [28]. The summed bicoherence is shown in figure 8(b). The peaks in the LFZF and MSEF frequency regions are clearly demonstrated.

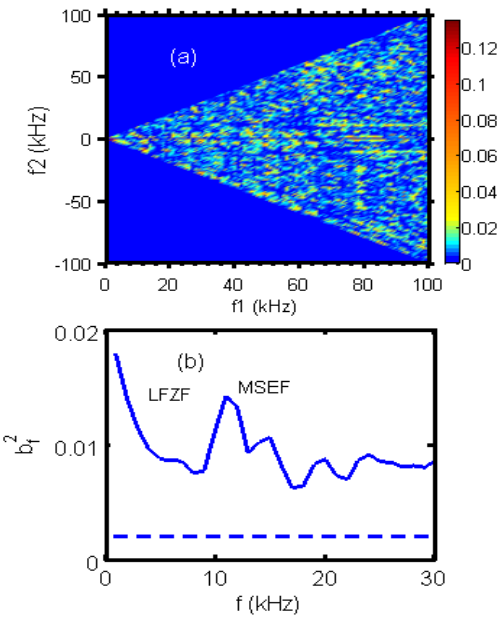

Fig.8. (color online) (a) The auto-bicoherence of the floating potential fluctuations, and (b) the summed bicoherence.

3.6 Nonlinear coupling of MSEFs to LFZFs

The new mechanism for the LFZF formation is the coupling of the MSEFs and LFZFs. This differs from the turbulence driving and deserves to be studied. Figure 9 gives the zoomed-in plot of figure 8(a). The squared auto-bicohence of the floating potential fluctuations in the frequency region of f_1*<30 kHz*, and f_2*=-30- + 30 kHz* is presented. The higher values in the frequency region of f_1 *= 9 - 14 kHz*, f_2 *= ~0-4kHz*,

and $f = f_1 + f_2 \sim$ 0-4 *kHz* are apparently shown. The observation suggests that it is possible that the LFZFs are created through three wave coupling between MSEFs and LFZFs.

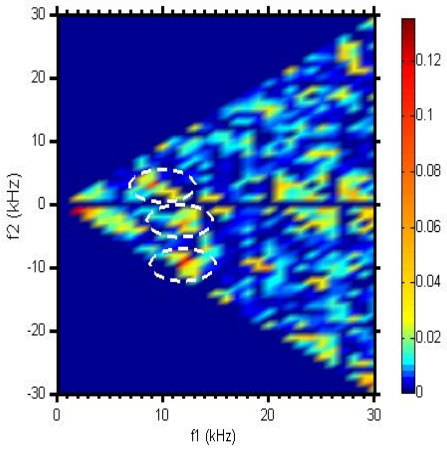

Fig.9. (color online) The auto-bicoherence of the floating potential fluctuations.

3.7 Turbulence envelope modulation

The modulations of MSEFs and LFZFs on turbulence are analyzed with the envelope analysis. The coherencies between the MSEFs and the turbulence envelope, and between the LFZF and turbulence envelope in various frequency bands presented in figure 10 (a) indicate that both LFZFs and MSEFs modulate the turbulence and that the MSEFs mainly regulate the turbulence of frequencies higher than 100 kHz and lower than 200 kHz. Whereas the LFZF mainly modulates the turbulence of frequencies lower than 100 kHz. The tendencies of the modulation from LFZF and MSEFs are similar in the frequency regime higher than 300 kHz. The corresponding phase shifts are close to $\pi/2$ and π between the MSEF and the turbulence envelope, and between the LFZF and the turbulence envelope in various frequency bands, respectively, as given in figure 10 (b). Here, f_C is the central frequency of the selected frequency band.

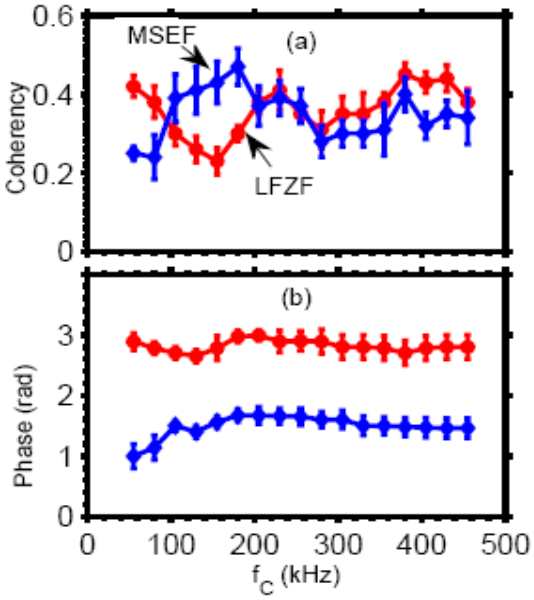

Fig 10 (color online) (a) The coherencies between the MSEFs and the turbulence envelopes, and between the LFZF and turbulence envelope in various frequency bands, and (b) Their corresponding phase shifts.

3.8 MSEF envelope modulation

The effects of LFZFs on MSEFs are exploited with the envelope analysis of the MSEFs. The waveforms of the LFZF and the envelope (shown in figure 11) show that the LFZF is well correlated with the MSEF envelope and the phase shifts between them is close to π. This analysis suggests that the LFZF modulates the MSEFs.

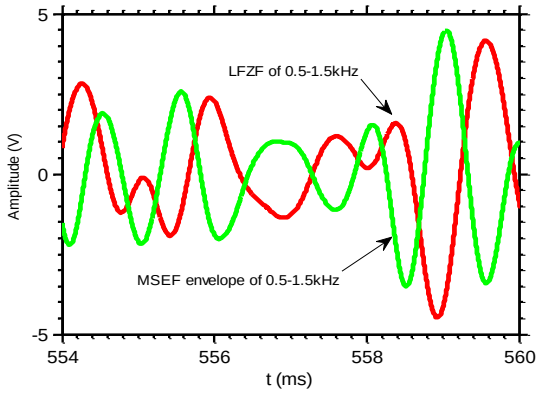

Fig.11. (color online) The waveforms of the LFZF and the turbulence envelopes.

4. Discussion and conclusion

The synchronization of GAMs and magnetic fluctuations is observed in the edge plasmas of the HL-2A tokamak. The new MSEFs, resulting from the synchronization and having components of dominant GAM and m/n=6/2 potential fluctuations, are found at the same frequency as that of the magnetic fluctuations of m/n=6/2. The MSEFs couple to turbulence and LFZFs. Both the MSEFs and the LFZFs modulate the turbulence while the MSEFs are regulated by the LFZFs.

This experiment is designed to measure the mode numbers of GAMs (n=0) and potential fluctuations (m/n=6/2) with the same frequency and the radial distribution of the MSEFs simultaneously and performed with multiple discharges and with similar plasma parameters. For this analysis, 20 shots have been used, among which17 shots show such a phenomenon unambiguously. Another example of the phase PDFs is provided in the figure 12. The analysis of the phase PDFs shows that the significant peaks in PDFs during the ECRH appear always, while the apparent peaks in PDFs before ECRH appear or disappear shot to shot.

The m/n=3/1 basic harmonic mode is not observed in the present experiments. This indicates that the m/n=6/2 mode does not come from the m/n=3/1 basic harmonic

mode. The turbulence-driven GAMs has close frequency with m/n=6/2 magnetic fluctuations. The synchronization of GAMs and magnetic fluctuations suggests that GAMs and magnetic fluctuations can transfer energy between each other through nonlinear synchronization. Therefore, the observation suggests that synchronization might contributes to the excitation of m/n=6/2 magnetic fluctuations. This can not be understood by the present theory. In this experiment, we also observed that the MSEFs interact with LFZFs and turbulence, suggesting that the synchronization contributes to the LFZF formation, and thus reduces turbulence level. The LFZF is a favorable for the L-H transitions [29]. Thus, we speculate that the synchronization can contribute to confinement regime transitions, especially L-H transitions. Note that the m/n=4/2 mode of f~12 kHz is not correlated with GAMs. The possible conjecture is that the q=2 rational surface is far away from the GAM location although the m/n=4/2 mode frequency is close to that of GAMs. The m/n=4/2 modes occur at the q=2 rational surface in the core plasmas while both the GAMs and the m/n=6/2 modes are localized in the edge plasmas. This difference between 4/2 and 6/2 modes gives a clue to

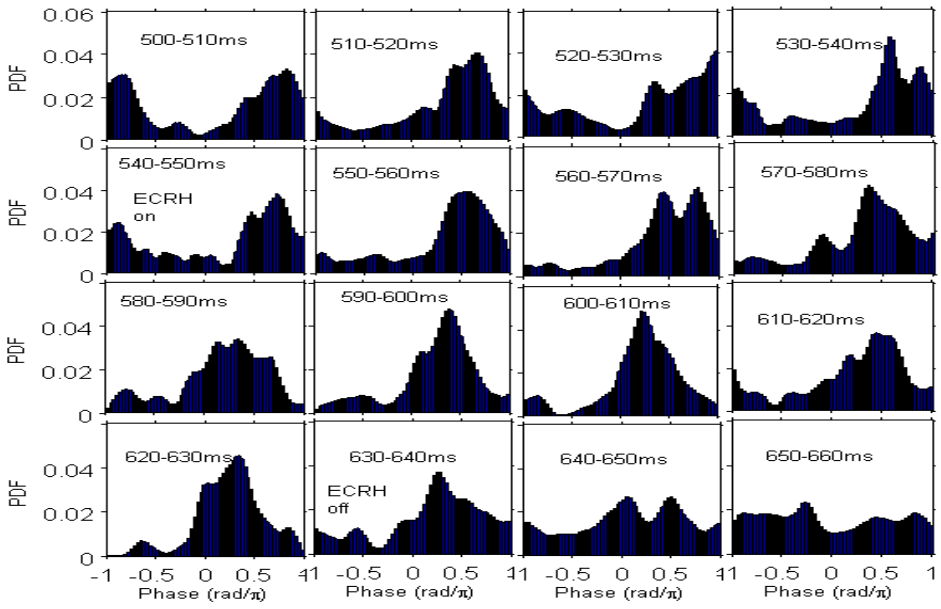

Fig. 12. (color online) The probability density functions of phase shifts between MSEFs and magnetic fluctuations at different time slices.

understand the mechanism that causes observed synchronization.

The observation provides a problem definition to study nonlinear interactions among magnetic islands and the low frequency zonal flows and GAMs. It has been theoretically pointed that the mean and zonal flows and magnetic island interact directly [30-32], e.g., the influence by the flow on island growth [33] and that by magnetic island on flow [34] have been reported. The indirect interactions between flows and islands have also been extensively studied. Here, *indirect* means the interaction between them via change of turbulence. That is, the energy of microscopic turbulence is transferred to tearing modes [35-38], so that the fluctuation intensity and the drive of zonal flows by turbulence can be reduced. The magnetic islands enhance the damping rate of zonal flows, so that they affect the intensities of flows and turbulence simultaneously [39]. These theoretical studies have focused on the impacts, which are given as averaged values on the magnetic surface, so that the sensitivity to the phase of magnetic perturbation has not attracted attentions much. It has also been pointed out that the fluctuation intensity is modulated with the same period as magnetic islands [35, 36], and an initial observation was reported [40]. Therefore, there can be a coupling effect between them, which is sensitive to the phase of the magnetic island. The fact that the zonal flow is synchronous with the island actually suggests that the zonal flows see the islands, and respond to the island with sensitivity to the phase.

This study of the interactions of LFZFs and GAMs and magnetic fluctuations suggest that the phase dynamics of magnetic fluctuations and zonal flows can contribute to the coherent structure formation, and thus control the transport and plasma confinement.

Acknowledgement:

The authors thank the Joint Data Analysis Workshop, organized by Profs. S.-I. Itoh, S. Inagaki, and K. Itoh held at Kyushu University, Japan, and the 2nd APTWG Conference held at Southwestern Institute of Physics, China, which provided opportunities for detailed and valuable discussion on this subject. This work is supported by the National Magnetic Confinement Fusion Science Program No.

2014GB108004, 2015GB106005 , 2013GB107001, 2014GB107000 and 2013GB112008; by the fund of State Key Laboratory of Advanced Electromagnetic Engineering and Technology in HUST (2016KF008); by the National Science Foundation of China, Nos. 11175060, 11375054, 91130031, 11505048 and 11320101005; by Grant-in-Aid for Scientific Research of JSPS (15H02155, 15H02335, 16H02442); by the Department of Energy 346 under Award No. DE-FG02-04ER54738 and by the WCI Program of the National Research Foundation of Korea funded by the Ministry of Education, Science and Technology of Korea [WCI 2009- 001].

Reference:

[1] Seanp Matt. et al., APJ, **754**, L26 (2012).

[2] Balbus S. A and Hawley J. F. APJ, **376**, 241(1991).

[3] Balbus S. A and Hawley J. F. Rev. Mode. Phys, **70**, 1,(1998).

[4] Aubert J and Fournier A. Nonlin. Processes Geophys, **18**, 657(2011).

[5] Biskamp D. Magnetic Reconnection in Plasmas, (Cambridge University Press, Cambridge, England, 2000).

[6] Kaw P. K, Valeo E. J, and Rutherford P. H. Phys. Rev.Lett. **43**, 1398 (1979).

[7] Itoh S-I, Itoh. K, and Yagi. M. Phys. Rev. Lett. **91**, 045003 (2003).

[8] Estrada T. et al, Nucl. Fusion, **47**, 305 (2007).

[9] Lin. Z et al., 25th IAEA fusion conference, TH/7-2, 13-18 October 2014, Saint Petersburg, Russia.

[10] Evans T. E. et al., Phys. Rev. Lett. **92**, 235003 (2004).

[11] Hasegawa A. et al., Phys. Rev. Lett. **59**, 1581 (1987).

[12] Diamond P. H. et al., Plasma Phys. Cont. Fusion **47**, R35 (2005).

[13] Winsor N. et al., Phys. Fluids **11**, 2448 (1968).

[14] Zhao K. J. et al., Phys. Rev. Lett. **96**, 255004 (2006)

[15] Robinson J. R. et al., Plasma Phys. Control. Fusion **54**, 105007(2012).

[16] Zhao K. J. et al., Nucl. Fusion, **55** (2015) 073022.

[17] Zhao K. J. et al., Nucl. Fusion, **56** (2016) 076005.

[18] Ida. K, et al., Phys. Rev. Lett. **88**, 015002 (2002).

[19] Tsui H. W. Y. et al., Phys. Rev. Lett. **70**, 2565 (1993).

[20] Tsui H. W. Y. et al., Phys. fluids B **5**, 1274 (1993).

[21] Pecora L. M, and Carroll T. L. Phys. Rev. Lett. **64**, 821 (1990).

[22] Pikovsky A， Rosemblum. M, and Kurths. J. Synchronization: A Universal Concept in Nonlinear Sciences, (Cambridge University Press, Cambridge, England, 2001).

[23] Acebr′on. J. A. et al., Rev. Mod. Phys **77**, 137(2005).

[24] Guo. Z. B and Diamond P. H. Phys. Rev. Lett. **114**, 14500296(2015).

[25] Zhao K. J. et al., Phys. Rev. Lett. **117**, 145002 (2016).

[26] Zhao. K. J. et al., Plasma Phys. Cont. Fusion **52**, 124008 (2010).

[27] Jha. R, Raju. D, and Sen. A. Phys. Plasmas, **13**, 082507 (2006).

[28] Xu. M. et al, Phys. Rev. Lett. **108**, 245001(2012).

[29] Zhao K. J. et al., Nucl. Fusion **53**, 123015 (2013).

[30] Wang. Z.X. et al., Phys. Rev. Lett. 103, 015004 (2009).

[31] Wang. Z.X. et al., Phys. Plasmas 16, 060703 (2009).

[32] Scott. B. D. New. J. Phys, 7, 92(2005).

[33] Smolyakov A. I. et al., Phys. Plasmas **2**, 1581 (1995).

[34] Shaing K. C, Phys. Plasmas **9**, 3470 (2002).

[35] Yagi M. et al., Nucl. Fusion **45**, 900(2005).

[36] Muraglia M. et al., Nucl.Fusion **49**, 055016(2009).

[37] Hu. Z. Q, et al., Nucl. Fusion 54, 123018 (2014).

[38] Hu. Z. Q, et al., Nucl. Fusion 56, 016012 (2016).

[39] Leconte M and Diamond P. H, Phys. Plasmas **18**, 082309 (2011).

[40] Zhao K. J. et al., Plasma flows and turbulence in the vicinity of magnetic islands in a toroidal plasma, presented at APTWG Meeting (Jeju Island, Korea, B04, 5. 22. 2013)